

# **Contractile work directly modulates mitochondrial protein levels in human engineered heart tissues**

Ronald Ng<sup>1</sup>, Lorenzo R. Sewanan<sup>1</sup>, Allison L. Brill<sup>2</sup>, Paul Stankey<sup>1</sup>, Xia Li<sup>1</sup>, Yibing Qyang<sup>3,4,5,6</sup>, Barbara E. Ehrlich<sup>2,7</sup>, Stuart Campbell<sup>1</sup>

<sup>1</sup> Department of Biomedical Engineering, Yale University, New Haven, CT

<sup>2</sup> Department of Cellular and Molecular Physiology, Yale University, New Haven, CT

<sup>3</sup> Yale Cardiovascular Research Center, Section of Cardiovascular Medicine, Department of Internal Medicine, Yale School of Medicine, New Haven, CT

<sup>4</sup> Department of Pathology, Yale School of Medicine, New Haven, CT

<sup>5</sup> Yale Stem Cell Center, Yale University, New Haven, CT

<sup>6</sup> Vascular Biology and Therapeutics Program, Yale School of Medicine, New Haven, CT

<sup>7</sup> Department of Pharmacology, Yale University, New Haven, CT

## **Key Words**

Engineered heart tissues, iPSC-derived cardiomyocytes, afterload, work loop

## **New and Noteworthy**

In this work, we present a novel bioreactor which allows for active length control of engineered heart tissues during extended tissue culture. Specific length transients were designed so that engineered heart tissues generated complete cardiac work loops. Chronic culture with various work loops suggests that mitochondrial mass and biogenesis is directly regulated by work output.

## **Running Title**

Contractile work directly modulates mitochondrial regulation

## **Correspondence**

Stuart G. Campbell  
215 Malone Engineering Center  
55 Prospect St.  
New Haven, CT 06511  
stuart.campbell@yale.edu

## **Abstract**

Engineered heart tissues (EHTs) have emerged as a robust in vitro model to study cardiac physiology. Although biomimetic culture environments have been developed to better approximate in vivo conditions, currently available methods do not permit full recapitulation of the four phases of the cardiac cycle. We have developed a bioreactor which allows EHTs to undergo cyclic loading sequences that mimic in vivo work loops. EHTs cultured under these working conditions exhibited enhanced concentric contractions but similar isometric contractions compared to EHTs cultured isometrically. EHTs that were allowed to shorten cyclically in culture had increased capacity for contractile work when tested acutely. Increased work production was correlated with higher levels of mitochondrial proteins and mitochondrial biogenesis; this effect was eliminated when tissues were cyclically shortened in the presence of a myosin ATPase inhibitor. Leveraging our novel in vitro method to precisely apply mechanical loads in culture, we grew EHTs under two loading regimes prescribing the same work output but with different associated afterloads. These groups showed no difference in mitochondrial protein expression. In loading regimes with the same afterload but different work output, tissues subjected to higher work demand exhibited elevated levels of mitochondrial protein. Our findings suggest that regulation of mitochondrial mass in cultured human EHTs is potently modulated by the mechanical work the tissue is permitted to perform in culture, presumably communicated through ATP demand. Precise application of mechanical loads to engineered heart tissues in culture represents a novel in vitro method for studying physiological and pathological cardiac adaptation.

## Introduction

The heart is a highly adaptable organ, capable of altering its properties over both short and long timescales. Cardiac output can be modulated within seconds to match an increased demand for oxygen such as during strenuous exercise. If increased demand is sustained over a prolonged period, the heart undergoes macroscopic and microscopic changes to achieve an adapted equilibrium. Macroscopic morphological alterations occur in the absence of cardiomyocyte proliferation and are due in large part to accumulated cellular and extracellular matrix modifications (1). Depending on the type of loading conditions, the left ventricle can dilate or thicken as a result of respective parallel or series addition of sarcomeres within each cardiomyocyte (1). Beyond the sarcomere, cardiomyocytes also modulate mitochondrial biogenesis (2). These changes in and outside of the sarcomere work in concert to maintain cardiac output while maximizing efficiency.

Although cardiac remodeling processes may be adaptive and help to maintain homeostasis, these changes may become maladaptive over time and contribute to the development of heart failure (3,4). Understanding the detailed mechanisms by which mechanical loads are transduced to cellular changes is therefore of critical importance but remains poorly understood (5). Progress has been elusive in part due to the difficulty of studying cardiomyocytes under precise loading conditions, whether *in vivo* or *in vitro*.

Human induced pluripotent stem cell derived cardiomyocytes (hiPSC-CMs) have emerged as an exciting *in vitro* method to study cardiac mechanotransduction. A major obstacle to using this model to its full potential is a lack of techniques for applying realistic mechanical stimuli to hiPSC-CMs during culture (6). HiPSC-CMs grown directly on plastic culture plates experience very high afterloads that approach isometric conditions. Prolonged culture of hiPSC-CMs on substrates with unphysiologically high

stiffnesses has been shown to reduce sarcomere organization, decrease electrical excitability, and promote mechanical dysfunction (7–9).

In contrast, 3D engineered myocardial constructs generated from hiPSC-CMs are typically grown between flexible posts or supports which allows hiPSC-CMs to experience physiological stiffness and shortening (10–12). Mechanical loading can be perturbed by altering the stiffness of tissue supports, after which chronic responses can be observed (13). Although these experiments have provided some insights, they have been limited to altering auxotonic loading of the tissues, which equates to simultaneous changes in multiple mechanical loading parameters, including shortening velocity, maximum sarcomere shortening, and elastic load. Consequently, it remains unclear which of these factors are the primary trigger that cause the resulting changes in cellular behavior.

Accordingly, we designed a system capable of delivering precise mechanical loads to engineered human myocardial samples under chronic culture conditions. Our efforts yielded a design that enables independent regulation of afterload and contractile work, allowing the impact of each factor on myocardial remodeling to be clearly observed. The system was also designed to allow tissues to be transferred from chronic dynamic culture to an apparatus for acute mechanical testing. We used the system to investigate the roles of mechanical load and contractile work in regulation of mitochondrial biogenesis, connecting cellular remodeling to specific mechanical inputs.



## Methods

### *HiPSC culture and differentiation*

Human induced pluripotent stem cells were acquired from Coriell Institute for Medical Research (GM23338). HiPSC colonies were maintained on Matrigel-coated plates (BD Biosciences) and in mTeSR-1 media (StemCell Technologies) until confluent. Once confluent, cardiac differentiation was induced using previously published methods with slight alterations (14). Cells were cultured in RPMI with 1x B27minus insulin (Thermo Fisher Scientific) and 12.5  $\mu$ M CHIR99021 (StemCell Technologies) for 24 hours. Media was removed and replaced with fresh RPMI with B27 minus insulin. After 48 hours of culture, fresh RPMI with B27 minus insulin containing 5 $\mu$ M IWP (StemCell Technologies) was added to the cells. After this, media was refreshed with RPMI with B27 minus insulin every other day until day 9, after which RPMI containing B27 (with insulin) was used. Cardiomyocytes were cultured until day 14 at which point they were dissociated and seeded onto decellularized porcine myocardium.

### *EHT generation*

Engineered Heart Tissues (EHTs) were generated via previously published methods described in *Schwan et al.* 2016 (15). Briefly, porcine hearts were dissected and blocks of the left ventricular free wall were removed and frozen. Blocks were sectioned into 150 $\mu$ m thick slices parallel to the muscle fiber direction. Slices were then incubated in a lysis buffer (10 mM Tris, 0.1% w/v EDTA, pH 7.4) for 2 hours before being attached to PTFE clips. Tissues were incubated in sodium dodecyl sulfate (0.5% w/v in PBS) for 40 minutes with gentle agitation before being incubated in DMEM + 10% FBS with 2x Penicillin-Streptomycin overnight. Cardiomyocytes were dissociated via incubation with TrypLE (ThermoFisher Scientific) and cocultured with human adult cardiac fibroblast at a ratio of 10:1 before being seeded

onto the scaffold at a density of 1.5 million cells per scaffold. EHTs were cultured for 1 week under isometric conditions before being used for experiments.

### *Bioreactor design and fabrication*

A schematic of the bioreactor with associated control systems can be seen in Figure 1A. An MSP-EXP430F5529LP (Texas Instruments) was used to coordinate electrical stimulation with position control. Biphasic pulses were applied using a custom-built circuit composed of a linear voltage regulator (Texas Instruments) and an H-bridge (Texas Instruments) and parallel carbon plates. Simultaneously, a prescribed analog signal was generated using a digital to analog converter (Texas Instruments) and was fed into a Pluto Servo Drive Controller (Ingenia). A predefined analog signal specified the position of a voice coil linear actuator (Ingenia) which in turn drove a stainless-steel spring arm. Accurate position control was verified through an analog feedback signal. The spring arm was affixed to a custom designed 3D printed adapter (Formlabs Dental SG resin) which fit over a 6 well plate and allowed 6 EHTs to be shortened in parallel. EHTs were ejected from their Teflon frames and attached to a fixed arm and spring arm. EHTs were then cultured at a frequency of 1 Hz for one week before undergoing mechanical characterization and protein analysis (Fig 1B).

### *Mechanical Testing*

After one week of dynamic culture, mechanical testing was performed on a custom-built setup. Tissues were tested in Tyrode's solution (140 mM NaCl, 5.4 mM KCl, 1 mM  $MgCl_2$ , 25 mM HEPES, 10 mM glucose, and 1.8 mM  $CaCl_2$ ; pH adjusted to 7.3) and active force was measured with a force transducer (World Precision Instruments KG7) attached to one end of the EHT. On the other end, tissues were

attached to a high speed length controller (Aurora 322C). Isometric twitch records were collected for each EHT, as well as twitch records under user-defined shortening protocols. Peak isometric force, time from stimulus to peak force (isometric TtP), time from peak force to 50% relaxation (isometric RT50) were calculated from isometric twitch records. Peak force under shortening conditions, normalized force-time integral, and maximum instantaneous power were calculated from twitch records collected during EHT shortening. Normalized force – time integral was calculated by integrating the area under the force transient after normalization to that EHT's maximum isometric force. Maximum power was calculated by multiplying the shortening velocity and force at each collection time point within the twitch record. Contractile work was calculated by integrating the area enclosed by the force-length relation throughout the duration of the twitch. Calcium transients were recorded using Fura-2, a calcium-sensitive dye. After loading EHTs with Fura-2, transients were recorded under excitations centered around 340nm or 380nm wavelength light. Custom MATLAB post processing routines calculated the ratiometric response at each time point.

### *Western Blot*

After mechanical testing, EHTs were homogenized in RIPA buffer (Santa Cruz Biotechnology, Dallas, Tx) supplemented with phosphatase inhibitor (Santa Cruz Biotechnology), sodium orthovanadate (Santa Cruz Biotechnology), protease inhibitor cocktail (Santa Cruz Biotechnology), and PMSF (Santa Cruz Biotechnology). Protein was separated on 4-20% Mini-PROTEAN TGX Gels (Bio-Rad, Hercules, CA) or NuPAGE 4-12% Bis-Tris Protein Gels (ThermoFisher) before being transferred to PVDF membrane (Millipore, Carrigtwohill, CO). Primary antibodies used include Tropomyosin-1 (product no. 3910s, Cell Signaling Technology), ATP5H (product no. Ab110275, Abcam), VDAC (Proteintech #55259-1-AP), TOM20 (Santa Cruz Biotechnology #sc-17764), PGC1 $\alpha$  (Cell Signaling Technology #2178), and PINK1 (Cell

Signaling Technology #6946) diluted to 1:1000. Samples were normalized to total protein using either Li-Cor Revert Total Protein Stain (Li-Cor) or Ponceau Red stain (Santa Cruz Biotechnology).

## Results

### *Effect of dynamic culture on contractile properties of EHTs*

EHTs were prepared as previously described and cultured under isometric conditions for 7 days before being loaded into the bioreactor (Fig 1A) (15). Constructs were subsequently cultured under either working conditions (WC, made to shorten during each contraction) or isometric conditions (IC, constant length) for an additional seven days (Fig 1B). Tissues were cultured at similar diastolic lengths, but working EHTs underwent a prescribed shortening protocol during systole and were then re-stretched to their original length in early diastole (Fig 2A). After conditioning, EHTs underwent acute mechanical characterization. This enabled an examination of the effects of chronic mechanical loading on acute muscle behavior.

We first investigated the effects of chronic conditioning on the acute isometric force generating capacity of EHTs (Fig 2B). We found that the peak isometric force produced by WC EHTs showed no significant difference relative to IC EHTs (Fig 2C, 2D). Contraction and relaxation kinetics were unchanged, and no differences were observed in time to peak force (TTP) or time from peak force to 50 percent relaxation (RT50) between the two groups (Fig 2E, 2F). Additionally, calcium transients were unchanged between culture conditions (Fig 2H-K).

EHTs from either culture condition had similar amounts of tropomyosin which suggests a lack of hypertrophy as a result of working culture (Sup Fig A). Working culture did not appear to alter other aspects of EHT function. The Frank-Starling and force-frequency responses were unchanged between culture conditions (Sup Fig B, C).

Next, we examined the effect of chronic loading on acute EHT behavior while performing working contractions. Both WC and IC EHTs were tested under the same muscle shortening regime that was used for chronic working culture (Fig 2L). Whereas maximum force achieved during shortening was not significantly different between isometric and working culture, there was a trend towards WC EHTs generating increased peak force during shortening (Fig 2M, N). Working culture EHTs had a 60% increased normalized force-time integral (\* $p < 0.05$ ) and a 62% increase in instantaneous maximum power (\* $p < 0.05$ ; Fig 2O, 2P).

These findings suggest that when EHTs are made to contract concentrically during culture, adaptations occur that allow the muscle to generate increased force and power during shortening compared with statically cultured EHTs. Adaptation does not come at the expense of isometric force capacity, as tissues in either culture condition had comparable isometric twitches. These adaptations do not appear to be a result of altered calcium handling, as calcium transients were unchanged between culture conditions.

#### *Mitochondrial biogenesis is driven primarily through contractile work*

The Fenn effect describes the increased contractile work performed by a shortening muscle versus a muscle held at a fixed length (16). From principle of energy conservation, this increased work output must be matched by increased substrate consumption. We hypothesized that sustained increased contractile work demanded of WC tissues would drive mitochondrial biogenesis as a response to increased ATP utilization. Fig 3A shows representative work loops done in culture, confirming that WC EHTs perform increased work compared to IC EHTs. When both groups were subjected to the culture shortening transients during acute mechanical testing, WC EHTs were able to generate 42% more contractile work compared with IC EHTs (Fig 3B). WC EHTs expressed 3.20 fold higher levels of PGC1 $\alpha$  which indicates increased mitochondrial biogenesis (\* $p < 0.05$ ; Fig 3C). Correspondingly, WC EHTs

contained significantly higher levels of several mitochondrial proteins compared to IC EHTs: ATP synthase (ATP5H) [ 3.27 fold increase;  $^{**}p < 0.01$ ], mitochondrial calcium uniporter (MCU)[ 8.37 fold increase;  $^{**}p < 0.01$ ], voltage-dependent anion channel (VDAC) [ 2.24 fold increase;  $^{*}p < 0.05$ ], mitochondrial import receptor subunit20 (TOM20) [ 1.63 fold increase;  $^{**}p < 0.01$ ] – suggesting an increase in mitochondrial mass (Fig 3C-G). These changes mirror the adaptation to shortening observed in WC twitches.

#### *Inhibition of the myosin ATPase mitigates increased mitochondrial biogenesis associated with dynamic culture*

We next investigated whether the increases in mitochondrial mass were driven primarily through increases in ATP utilization due to increased work done, or through other factors such as strain or afterload.

To determine whether mitochondrial biogenesis was driven through strain-dependent pathways, we cultured WC EHTs with the myosin ATPase inhibitor blebbistatin. This allowed EHTs to experience the same length changes (strains) as before, but with reduced external work production due to inhibition of the myosin ATPase (Fig 4A). After one week of culture, EHTs were probed for markers of mitochondrial biogenesis, general mitochondrial proteins, and mitophagy. Similar to the previous experiment, untreated WC EHTs demonstrated 2.24-fold higher levels of PGC1 $\alpha$  compared to untreated IC EHTs ( $^{*}p < 0.05$ ; Fig 4B). Blebbistatin decreased levels of PGC1 $\alpha$  by 73.6% in WC EHTs, suggesting the increase in mitochondrial biogenesis is dependent on work done in culture rather than due to changes in length ( $^{**}p < 0.01$ ; Fig 4B).

Blebbistatin also decreased the levels of mitochondrial proteins in treated WC EHTs compared to untreated WC EHTs – ATP5H [46% decrease ; \* $p < 0.05$ ], MCU [ 48% decrease; \* $p < 0.05$ ], VDAC [62% decrease; \*\*\* $p < 0.001$ ], TOM20 [41% decrease; \* $p < 0.05$ ] (Fig 4C-F). There was a significant interaction in the levels of PINK1, a marker for mitophagy, between blebbistatin and culture conditions (Fig 4G). Working culture EHTs tended to reduce protein levels of PINK, and these trends were reversed with blebbistatin. These data suggest that EHTs respond to increased work demand by increasing mitochondrial protein levels through a combination of increased mitochondrial biogenesis and decreased mitophagy. Decreasing force production while maintaining the length changes experienced by the EHTs mitigates this response, suggesting that muscle shortening in and of itself is not a direct driver of increased mitochondrial biogenesis in working culture EHTs.

#### *Mitochondrial protein expression change occurs independently of experienced afterload*

We next developed a length transient which maintained a similar maximal afterload but with increased work output compared to isometric culture. This was achieved by delaying shortening until peak afterload was achieved (Figure 5A). Delayed shortening (DSC) EHTs experienced 105% of isometric force (Figure 5B) and generated 58.10 nJ of contractile work per cycle (Figure 5C). DSC EHTs had 1.4 fold higher levels of ATP synthase subunit d compared to isometric EHTs. (\* $p < 0.05$ ; Fig5D). These data suggest that mitochondrial biogenesis is driven primarily through contractile work (ATP usage) rather than afterload or amount shortened.

Next, two unique length transients were developed to further dissociate the effects of afterload and contractile work on mitochondrial biogenesis (Figure 6A). High afterload (HA) EHTs reached 87% of isometric force and were shortened by 2% of resting length (Fig 6B, 6C). Low afterload (LA) EHTs reached 40% of isometric force and were shortened by 6% of resting length (Fig 6D, 6E). Two length transients resulted in similar amounts of work being done, but EHTs experienced significantly different afterloads

under either condition (Fig 6F, 6G). Interestingly, EHTs performed equally well in acute tests of either shortening regime, irrespective of the chronic shortening they experienced in culture (Fig 6H, 6I). This suggests that once EHTs are adapted to either chronic HA or LA culture, the other shortening regime is within the range of acute adaptation. This is in contrast to the first experiment in which isometrically cultured EHTs generated significantly less work and force when tested acutely under shortening conditions. ATP synthase content (shown above to correlate closely with expression of other major mitochondrial proteins) was not significantly different between the 2 groups ( $p = 0.14$ ), supporting the hypothesis that regulation of mitochondria is primarily sensitive to the amount of contractile work done by the tissue, and relatively insensitive to the process path (Fig 6J).

## **Discussion**

A long-standing concern with utilizing hiPSC derived cardiomyocytes for cardiac disease modeling is the relative metabolic immaturity of hiPSC derived cardiomyocytes (19). Compared to native adult cardiomyocytes, hiPSC-CMs more closely resemble fetal cardiomyocytes with a reduced density of mitochondria and more heavy reliance on mitochondria-independent ATP synthesis (glycolysis) (20,21). However, this makes hiPSC-CMs a potentially useful model for studying mitochondrial regulation. Mitochondrial density has been shown to improve when hiPSC-CMs were cultured under more physiological conditions such as on aptly stiff hydrogels or in 3D engineered heart tissues (22,23). Compared to isometric culture, cardiomyocytes formed into EHTs experience both altered shortening profiles as well as changes in contractile work produced (22). Therefore, from those data alone it is unclear whether mitochondrial biogenesis is driven primarily by strain-sensitive pathways or through regulatory mechanisms that seek to match ATP production to demand.

A cardiac cycle is composed of four parts: isovolumetric contraction, ejection, isovolumetric relaxation, and filling. When left ventricular pressure is plotted as a function of volume, the area within the



resultant loop represents the work done by the heart. In a one-dimensional system, force and length are analogs of pressure and volume. Critical to composing complete work loops in this analog system is the combination of isometric, concentric, and eccentric contractions to resemble phases of the cardiac cycle. Current methods of dynamic mechanical stimulation of engineered heart tissues utilize flexible boundary conditions to provide auxotonic loading conditions (11). Post stiffness can be altered in a variety of ways – additional curing agent/curing time, adjustable braces, magnetic resistance – however these methods do not allow adjustments within a single cardiac cycle (13,24–26). EHTs cultured using these methods only experience ejection and filling phases, and physiological work loops are not formed. Additionally, this results in the coupling of afterload and shortening velocity – increased post stiffness increases the resistance to contraction while simultaneously restricting the velocity of shortening. In contrast, we utilized a non-commutated DC linear actuator for active control of the tissue length. This enabled us to administer both isometric loading to EHTs as well as complete work loops. Precise dynamic length control also allowed for independent modulation of diastolic length, afterload, and shortening velocity.

Ulmer *et al.* compared mitochondrial content in cardiomyocytes grown in 2D versus 3D culture, finding that 3D culture (which permitted more sarcomere shortening and hence mechanical work) resulted in greater mitochondrial density and maturation (22). In addition to increased work output, 3D culture also provides different biomechanical cues than 2D culture which may influence metabolic maturation. Our observations that 3D working EHTs had an increased amount of mitochondrial proteins compared to 3D isometric EHTs furthers the hypothesis that ATP consumption is the primary driver of metabolic maturation. EHTs showed functional adaptation to working culture, as evidenced by trained EHTs generating larger normalized force-time integrals and reaching higher maximum power outputs compared to non-trained EHTs subjected to the same shortening profile. Interestingly, these improvements occurred in the absence of a difference in peak force generation. This suggests that

increased power generation is not a result of hypertrophy, but rather due to accelerated crossbridge kinetics better able to generate force during shortening. Comparable levels of tropomyosin between groups also suggest a lack of sarcomerogenesis.

Unique to our system is the ability to impose a prescribed length transient independent of load. We leveraged this advantage to investigate the relative effects of stress and strain sensitive pathways versus ATP consumption. We found that strain-sensitive pathways were not the primary effector, as regulation of mitochondrial biogenesis was attenuated by the application of a myosin ATPase inhibitor despite still maintaining a similar shortening profile.

A separate experiment demonstrated that stress-sensitive pathways also did not seem to be a major effector. Significant differences in ATP synthase levels were observed in two length transients that resulted in similar maximal afterloads. Similar to previous experiments, EHTs which generated increased mechanical work during culture had higher levels of mitochondrial protein.

Next we sought to modulate shortening profiles independently of contractile work. Active control of EHT length allowed generation of two culture conditions, each with different shortening profiles and afterloads, but requiring similar amounts of mechanical work. EHTs cultured under these two conditions had similar levels of ATP synthase, supporting the hypothesis that mitochondrial biogenesis is augmented primarily in response to increased ATP utilization.

Although we were able to implement physiologically similar culture work loops, our system is still short of reproducing the native myocardial environment. In an *in vivo* heart, shortening only occurs when wall tension increases enough to overcome aortic pressure, and blood is ejected (27). Physiological blood pressure requires this wall tension to remain sufficiently high through the entire contraction. In contrast, our bioreactor prescribes the length of tissue irrespective of tension. Due to the variability in strength

and kinetics of active contractions, some EHTs experienced unphysiologically low tension during the relengthening phase of the cycle. In future iterations, this artifact could be mitigated by implementing adaptable length transients controlled by individual EHT force feedback.

In this work, we developed a novel bioreactor in order to apply precise mechanical perturbations to engineered heart tissues during chronic culture. We demonstrated that regulation of mitochondrial protein expression was dependent on the amount of work done by the tissue but was independent of experienced afterload. Future research will focus on identifying molecular regulators of these pathways. This study provides the groundwork to further investigate cardiac mechanotransduction in physiology and pathophysiology.

## Figure Captions

**Figure 1) Bioreactor schematic and experimental flow chart. (A)** Human induced pluripotent stem cell derived cardiomyocytes (hiPSC-CMs) are seeded onto decellularized porcine myocardium fixed onto Teflon clip and frame system. Engineered heart tissues (EHTs) are then removed from the frame and loaded into bioreactor. Exploded side view demonstrating the fixed arm (left side), and the spring arm (right side) being deformed by the voice coil actuator causing EHT length changes. Six pairs of arms are arranged to fit over a regular six well tissue culture plate, and a “plunger” is used to allow the voice coil to control all of them in parallel. An MSP430 microcontroller is used to synchronize electrical stimulation and length control. **(B)** After 14 days of cardiac differentiation, hiPSC-CMs are used to construct EHTs. EHTs are cultured isometrically for seven days to allow for tissue remodeling. EHTs are then loaded onto the bioreactor and cultured for an additional seven days under a specified shortening protocol. At the end of this period, EHTs are removed from the bioreactor and are acutely exposed to a variety of shortening protocols while the force response is recorded.

**Figure 2) Engineered Heart Tissues adapt to shortening culture conditions while maintaining isometric force generating capabilities. (A)** Position of the spring arm throughout a single culture cycle. A negative position indicates the spring arm moving closer towards the fixed arm representing EHT shortening. **(B)** Representative transients of tissue length during acute isometric testing after seven days of culture under chronic conditions. **(C)** Representative force twitches collected during acute isometric testing. **(D-F)** Culture conditions had no significant effect on peak force or twitch kinetics produced during isometric contraction. **(H)** Representative calcium transients collected during acute isometric testing. **(I-K)** Culture conditions had no significant effect on calcium transients produced during isometric contraction. **(L)** Representative transients of tissue length during acute shortening testing after seven days of culture under chronic conditions. **(M)** Representative force twitches collected during acute testing while EHTs underwent the shortening protocol (working culture) represented in Fig 2L. **(N)** EHTs from either culture

condition had no difference in peak force produced during shortening. **(O)** EHTs cultured under working culture conditions produced significantly higher normalized force time integrals compared to EHTs cultured under isometric conditions. Force was normalized to maximum isometric force. (\*P < 0.05 for 2-tailed unpaired t-test, n = 7 in each condition) **(P)** EHTs cultured under working culture conditions produced significantly higher instantaneous maximum power compared to EHTs cultured under isometric conditions. Power was calculated by multiplying force by instantaneous velocity at that time point. (\*P < 0.05 for 2-tailed unpaired t-test, n = 7 in each condition)

**Figure 3) Working culture conditioned EHTs are more effective at generating contractile work and have higher levels of mitochondrial proteins. (A)** Representative force twitches plotted against tissue length. Twitches were collected during acute testing and represent the shortening protocol that each tissue was cultured under. **(B)** Contractile work generated when EHTs from either group were acutely tested under working culture shortening transients. EHTs cultured under working culture conditions produced significantly higher contractile work compared to EHTs cultured under isometric conditions. (\*P < 0.05 for 2-tailed unpaired t-test, n = 7 in each condition) **(C-G)** Immunoblots probed for levels of PPAR $\gamma$  coactivator 1  $\alpha$  (PGC1 $\alpha$ ), ATP synthase (ATP5H), mitochondrial calcium uniporter (MCU), voltage-dependent anion channel (VDAC), mitochondrial import receptor subunit20 (TOM20) reveal significantly higher levels in EHTs cultured under working culture. (fold change normalized to isometric; \*p < 0.05, \*\*p < 0.01 for 2-tailed unpaired t-test, n = 4 isometric culture; n = 3 working culture)

**Figure 4) Increased levels of mitochondrial proteins in working culture EHTs are attenuated by a myosin ATPase inhibitor. (A)** Representative force twitches plotted against tissue length. Twitches were collected during acute testing and represent the shortening protocol that each tissue was cultured under. **(B-F)** PGC1 $\alpha$ , ATP5H, MCU, VDAC, TOM20 protein levels were significantly increased in EHTs cultured under working conditions compared to EHTs cultured isometrically. Blebbistatin treatment significantly reduced protein levels in working culture EHTs. **(G)** PINK1 protein levels showed significant

interaction between blebbistatin treatment and culture conditions. (fold change normalized to untreated isometric;  $n = 3, 3, 4, 4$  for IC, IC+blebbistatin, WC, WC+blebbistatin respectively, 2 way ANOVA with Tukey multiple comparisons test  $*p < 0.05$ ,  $**p < 0.01$ ,  $***p < 0.001$ ).

**Figure 5) Training regimes with similar peak afterloads but different work outputs, result in different levels of ATP synthase**

**(A)** Position of the spring arm through a single culture cycle. Delayed shortening culture (DSC) initiates shortening concurrent with peak tension, resulting in similar maximal afterload compared to isometric culture, but with increased contractile work. **(B)** Force twitches collected during acute testing demonstrate EHTs from either group experience similar maximal afterload. **(C)**

Representative force twitches plotted against tissue length. Twitches were collected during acute testing and represent the increased contractile work EHTs generated in DSC compared to IC. **(D)** EHTs cultured under DSC have increased immunoblot levels of ATP5H. (fold change normalized to isometric;  $*p < 0.05$  for 2-tailed unpaired  $t$ -test, IC [ $n = 6$ ], DSC [ $n = 4$ ]).

**Figure 6) EHTs subjected to different training regimes with similar work outputs, maintain similar levels of ATP synthase**

**(A)** Position of the spring arm throughout a single culture cycle. High afterload culture (HA) transient is delayed in time and of smaller magnitude compared to Low afterload culture (LA) which results in EHTs contracting against higher load. **(B)** Representative transients of tissue length during acute HA testing after seven days of culture under chronic conditions. **(C)** Representative force twitches collected during acute testing while EHTs underwent the shortening protocol represented in Fig 2B (HA). **(D)** Representative work loops collected during acute HA testing. **(E)** EHTs generated similar levels of contractile work irrespective of chronic culture conditions during acute HA testing. (HA culture  $n = 12$ , LA culture  $n = 11$ ) **(F)** Representative transients of tissue length during acute LA testing after seven days of culture under chronic conditions. **(G)** Representative force twitches collected during acute testing while EHTs underwent the shortening protocol represented in Fig 2F (LA). **(H)** Representative work loops collected during acute LA testing. **(I)** EHTs generated similar levels of contractile work

irrespective of chronic culture conditions during acute LA testing. (HA culture n = 12, LA culture n = 11)  
(J) EHTs from either culture condition had similar immunoblot levels of ATP synthase (ATP5H) (n = 8 in each condition).

**Supplemental Figure 1) (A)** Working culture did not significantly increase levels of tropomyosin. **(B)** Working culture did not significantly alter Frank-Starling response. **(B)** Working culture did not significantly alter force - frequency response.

Supplemental Figure 2) (A-C) Representative immunoblots for tropomyosin and ATP synthase (ATP5H) with associated Licor Revert Total Protein stains

Supplemental Figure 3) (A-C) Representative immunoblots for PCG1- $\alpha$ , ATP5H, MCU, VDAC, and TOM20, with associated Ponceau Red Total Protein STain

**Acknowledgements**

The authors wish to acknowledge Aydin Akyol for engineering design work on bioreactor components.

This work was supported in part by NSF 1653160 (to S.G.C) and NIH R01 HL131940 (to Y.Q.). L.R.S. was supported by an American Heart Association Predoctoral Fellowship, a P.D. Soros Fellowship for New Americans, and by a National Institutes of Health/National Institute of General Medical Sciences Medical Scientist Training Program Grant (T32GM007205).

**Disclosure:**

S.G.C. has equity ownership in Propria LLC, which has licensed technology used in the research reported in this publication. The other authors have stated that no conflicts exist.



1. Maillet M, van Berlo JH, Molkenstein JD. Molecular basis of physiological heart growth: fundamental concepts and new players. *Nat Rev Mol Cell Biol* [Internet]. 2013;14(1):38–48. Available from: <https://doi.org/10.1038/nrm3495>
2. Dorn GW, Vega RB, Kelly DP. Mitochondrial biogenesis and dynamics in the developing and diseased heart. *Genes Dev* [Internet]. 2015 Oct 1;29(19):1981–91. Available from: <http://genesdev.cshlp.org/content/29/19/1981.abstract>
3. J. MA, Eugene B. Hypertrophic Cardiomyopathy. *Circ Res* [Internet]. 2017 Sep 15;121(7):749–70. Available from: <https://doi.org/10.1161/CIRCRESAHA.117.311059>
4. M. ME, Luisa M. Dilated Cardiomyopathy. *Circ Res* [Internet]. 2017 Sep 15;121(7):731–48. Available from: <https://doi.org/10.1161/CIRCRESAHA.116.309396>
5. Saucerman JJ, Tan PM, Buchholz KS, McCulloch AD, Omens JH. Mechanical regulation of gene expression in cardiac myocytes and fibroblasts. *Nat Rev Cardiol* [Internet]. 2019;16(6):361–78. Available from: <https://doi.org/10.1038/s41569-019-0155-8>
6. Sewanan LR, Campbell SG. Modelling sarcomeric cardiomyopathies with human cardiomyocytes derived from induced pluripotent stem cells. *J Physiol* [Internet]. 2019 Jan 9;n/a(n/a). Available from: <https://doi.org/10.1113/JP276753>
7. Bhana B, Iyer RK, Chen WLK, Zhao R, Sider KL, Likhitpanichkul M, et al. Influence of substrate stiffness on the phenotype of heart cells. *Biotechnol Bioeng* [Internet]. 2010 Apr 15;105(6):1148–60. Available from: <https://doi.org/10.1002/bit.22647>
8. Heras-Bautista CO, Katsen-Globa A, Schloerer NE, Dieluweit S, Abd El Aziz OM, Peinkofer G, et al. The influence of physiological matrix conditions on permanent culture of induced pluripotent stem cell-derived cardiomyocytes. *Biomaterials* [Internet]. 2014 Aug 1 [cited 2020 Jan

8];35(26):7374–85. Available from:

<https://www.sciencedirect.com/science/article/pii/S0142961214005845>

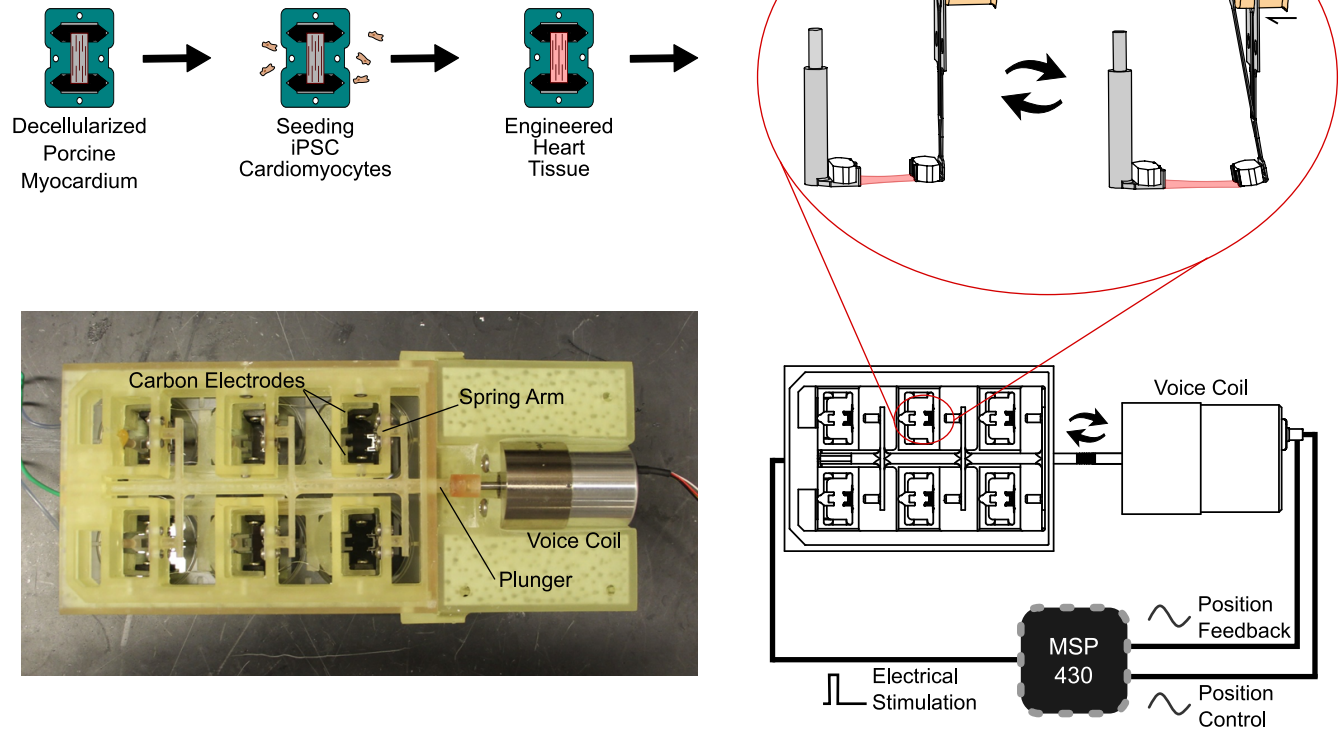
9. Sewanan LR, Schwan J, Kluger J, Park J, Jacoby DL, Qyang Y, et al. Extracellular Matrix From Hypertrophic Myocardium Provokes Impaired Twitch Dynamics in Healthy Cardiomyocytes. *JACC Basic to Transl Sci* [Internet]. 2019 Aug 1;4(4):495 LP – 505. Available from: <http://basictranslational.onlinejacc.org/content/4/4/495.abstract>
10. Jackman CP, Carlson AL, Bursac N. Dynamic culture yields engineered myocardium with near-adult functional output. *Biomaterials* [Internet]. 2016 Dec 1 [cited 2020 Jan 8];111:66–79. Available from: <https://www.sciencedirect.com/science/article/pii/S0142961216305269?via%3Dihub>
11. Schaaf S, Shibamiya A, Mewe M, Eder A, Stöhr A, Hirt MN, et al. Human Engineered Heart Tissue as a Versatile Tool in Basic Research and Preclinical Toxicology. *PLoS One* [Internet]. 2011 Oct 20;6(10):e26397. Available from: <https://doi.org/10.1371/journal.pone.0026397>
12. Nunes SS, Miklas JW, Liu J, Aschar-Sobbi R, Xiao Y, Zhang B, et al. Biowire: a platform for maturation of human pluripotent stem cell–derived cardiomyocytes. *Nat Methods* [Internet]. 2013;10(8):781–7. Available from: <https://doi.org/10.1038/nmeth.2524>
13. Leonard A, Bertero A, Powers JD, Beussman KM, Bhandari S, Regnier M, et al. Afterload promotes maturation of human induced pluripotent stem cell derived cardiomyocytes in engineered heart tissues. *J Mol Cell Cardiol* [Internet]. 2018 May 1 [cited 2019 Feb 28];118:147–58. Available from: <https://www.sciencedirect.com/science/article/pii/S0022282818300889?via%3Dihub>
14. Ng R, Manring H, Papoutsidakis N, Albertelli T, Tsai N, See CJ, et al. Patient mutations linked to arrhythmogenic cardiomyopathy enhance calpain-mediated desmoplakin degradation. *JCI Insight*

[Internet]. 2019;4(14). Available from: <https://doi.org/10.1172/jci.insight.128643>

15. Schwan J, Kwaczala AT, Ryan TJ, Bartulos O, Ren Y, Sewanan LR, et al. Anisotropic engineered heart tissue made from laser-cut decellularized myocardium. *Sci Rep* [Internet]. 2016;6:32068. Available from: <http://www.nature.com/articles/srep32068>
16. Fenn WO. A quantitative comparison between the energy liberated and the work performed by the isolated sartorius muscle of the frog. *J Physiol* [Internet]. 1923 Dec 28;58(2–3):175–203. Available from: <https://doi.org/10.1113/jphysiol.1923.sp002115>
17. Veigel C, Molloy JE, Schmitz S, Kendrick-Jones J. Load-dependent kinetics of force production by smooth muscle myosin measured with optical tweezers. *Nat Cell Biol*. 2003;5(11):980–6.
18. Smith DA, Geeves MA. Strain-dependent cross-bridge cycle for muscle. *Biophys J* [Internet]. 1995;69(2):524–37. Available from: [http://dx.doi.org/10.1016/S0006-3495\(95\)79926-X](http://dx.doi.org/10.1016/S0006-3495(95)79926-X)
19. Matsa E, Burrridge PW, Wu JC. Human Stem Cells for Modeling Heart Disease and for Drug Discovery. *Sci Transl Med* [Internet]. 2014 Jun 4;6(239):239ps6 LP-239ps6. Available from: <http://stm.sciencemag.org/content/6/239/239ps6.abstract>
20. Xiulan Y, Lil P, E. MC. Engineering Adolescence. *Circ Res* [Internet]. 2014 Jan 31;114(3):511–23. Available from: <https://doi.org/10.1161/CIRCRESAHA.114.300558>
21. Ronaldson-Bouchard K, Ma SP, Yeager K, Chen T, Song LJ, Sirabella D, et al. Advanced maturation of human cardiac tissue grown from pluripotent stem cells. *Nature* [Internet]. 2018;556(7700):239–43. Available from: <http://dx.doi.org/10.1038/s41586-018-0016-3>
22. Ulmer BM, Stoeckl A, Schulze ML, Patel S, Gucek M, Mannhardt I, et al. Contractile Work Contributes to Maturation of Energy Metabolism in hiPSC-Derived Cardiomyocytes. *Stem Cell Reports*. 2018;10(3):834–47.

23. Lyra-Leite DM, Andres AM, Cho N, Petersen AP, Ariyasinghe NR, Kim SS, et al. Matrix-guided control of mitochondrial function in cardiac myocytes. *Acta Biomater* [Internet]. 2019 Oct 1 [cited 2020 Jan 8];97:281–95. Available from:  
<https://www.sciencedirect.com/science/article/pii/S1742706119305549>
24. Rodriguez ML, Werner TR, Becker B, Eschenhagen T, Hirt MN. Magnetics-Based Approach for Fine-Tuning Afterload in Engineered Heart Tissues. *ACS Biomater Sci Eng*. 2019;5(7):3663–75.
25. Hirt MN, Sorensen NA, Bartholdt LM, Boeddinghaus J, Schaaf S, Eder A, et al. Increased afterload induces pathological cardiac hypertrophy: a new in vitro model. *Basic Res Cardiol*. 2012 Nov;107(6):307.
26. Boudou T, Legant WR, Mu A, Borochin MA, Thavandiran N, Radisic M, et al. A microfabricated platform to measure and manipulate the mechanics of engineered cardiac microtissues. *Tissue Eng Part A*. 2012 May;18(9–10):910–9.
27. Wiggers CJ. STUDIES ON THE CONSECUTIVE PHASES OF THE CARDIAC CYCLE. *Am J Physiol* Content [Internet]. 1921 Jul 1;56(3):415–38. Available from:  
<https://doi.org/10.1152/ajplegacy.1921.56.3.415>

A



B

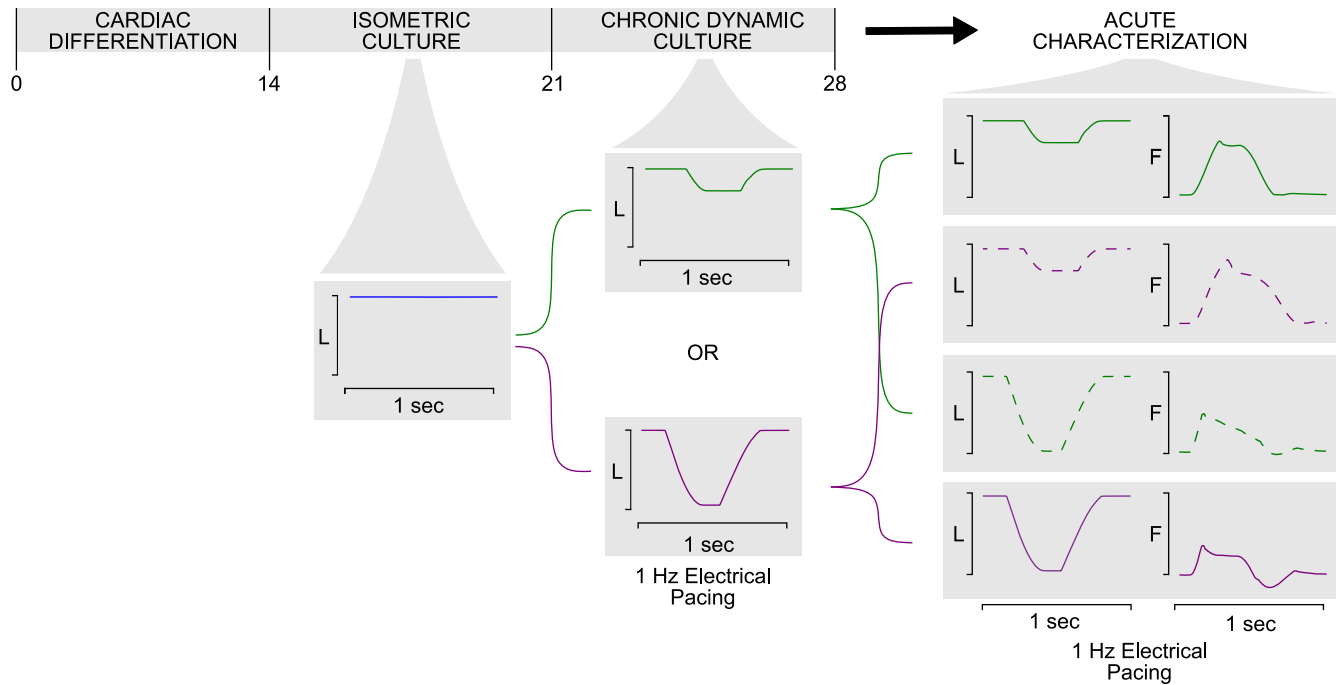


**Figure 1) Bioreactor schematic and experimental flow chart. (A)** Human induced pluripotent stem cell derived cardiomyocytes (hiPSC-CMs) are seeded onto decellularized porcine myocardium fixed onto Teflon clip and frame system. Engineered heart tissues (EHTs) are then removed from the frame and loaded into bioreactor. Exploded side view demonstrating the fixed arm (left side), and the spring arm (right side) being deformed by the voice coil actuator causing EHT length changes. Six pairs of arms are arranged to fit over a regular six well tissue culture plate, and a "plunger" is used to allow the voice coil to control all of them in parallel. An MSP430 microcontroller is used to synchronize electrical stimulation and length control. **(B)** After 14 days of cardiac differentiation, hiPSC-CMs are used to construct EHTs. EHTs are cultured isometrically for seven days to allow for tissue remodeling. EHTs are then loaded onto the bioreactor and cultured for an additional seven days under a specified shortening protocol. At the end of this period, EHTs are removed from the bioreactor and are acutely exposed to a variety of shortening protocols while the force response is recorded.

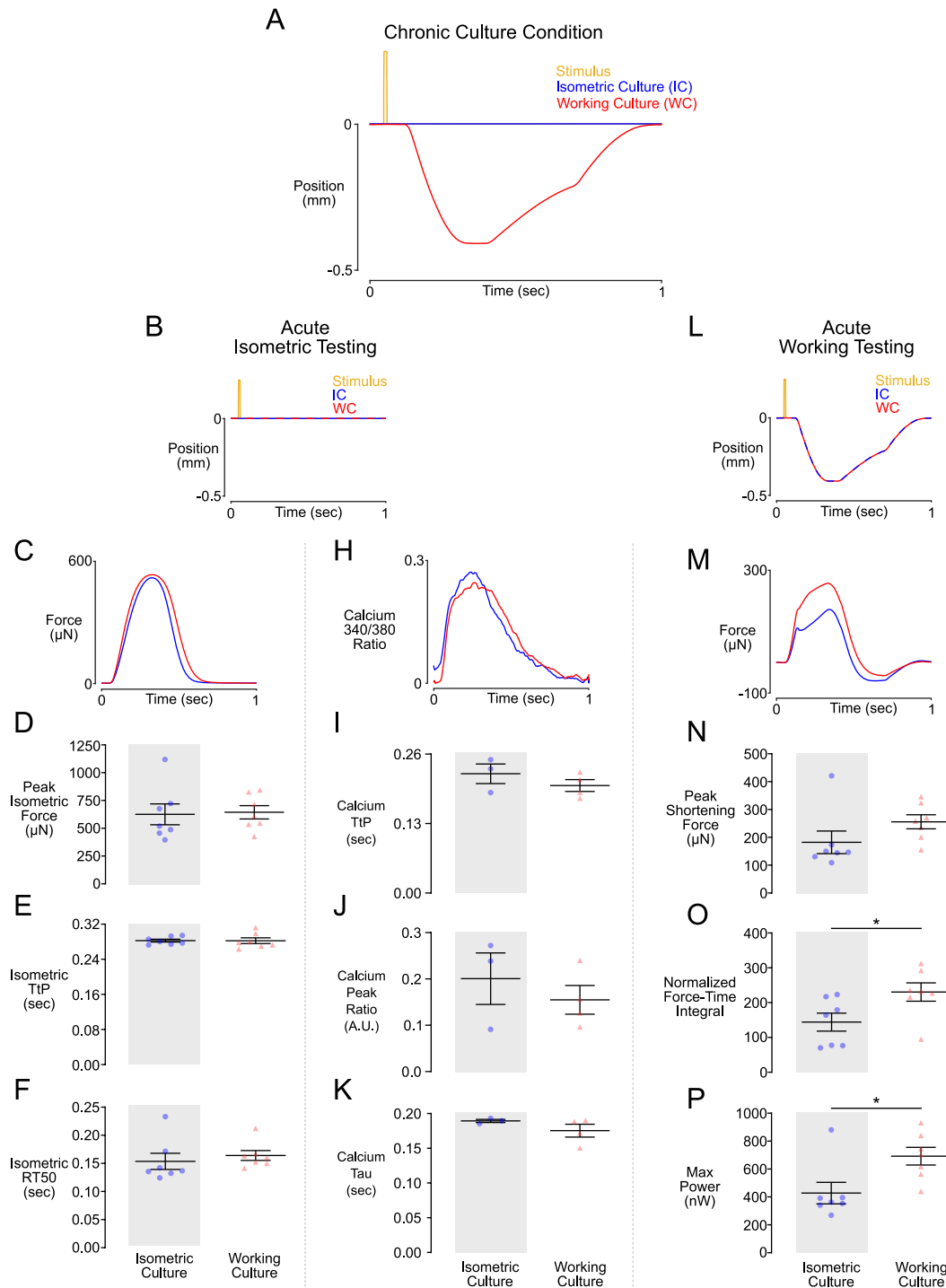


**Figure 2) Engineered Heart Tissues adapt to shortening culture conditions while maintaining isometric force generating capabilities.** (A) Position of the spring arm throughout a single culture cycle. A negative position indicates the spring arm moving closer towards the fixed arm representing EHT shortening. (B) Representative transients of tissue length during acute isometric testing after seven days of culture under chronic conditions. (C) Representative force twitches collected during acute isometric testing. (D-F) Culture conditions had no significant effect on peak force or twitch kinetics produced during isometric contraction. (H) Representative calcium transients collected during acute isometric testing. (I-K) Culture conditions had no significant effect on calcium transients produced during isometric contraction. (L) Representative transients of tissue length during acute shortening testing after seven days of culture under chronic conditions. (M) Representative force twitches collected during acute testing while EHTs underwent the shortening protocol (working culture) represented in Fig 2L. (N) EHTs from either culture condition had no difference in peak force produced during shortening. (O) EHTs cultured under working culture conditions produced significantly higher normalized force time integrals compared to EHTs cultured under isometric conditions. Force was normalized to maximum isometric force. (\* $P < 0.05$  for 2-tailed unpaired t-test,  $n = 7$  in each condition) (P) EHTs cultured under working culture conditions produced significantly higher instantaneous maximum power compared to EHTs cultured under isometric conditions. Power was calculated by

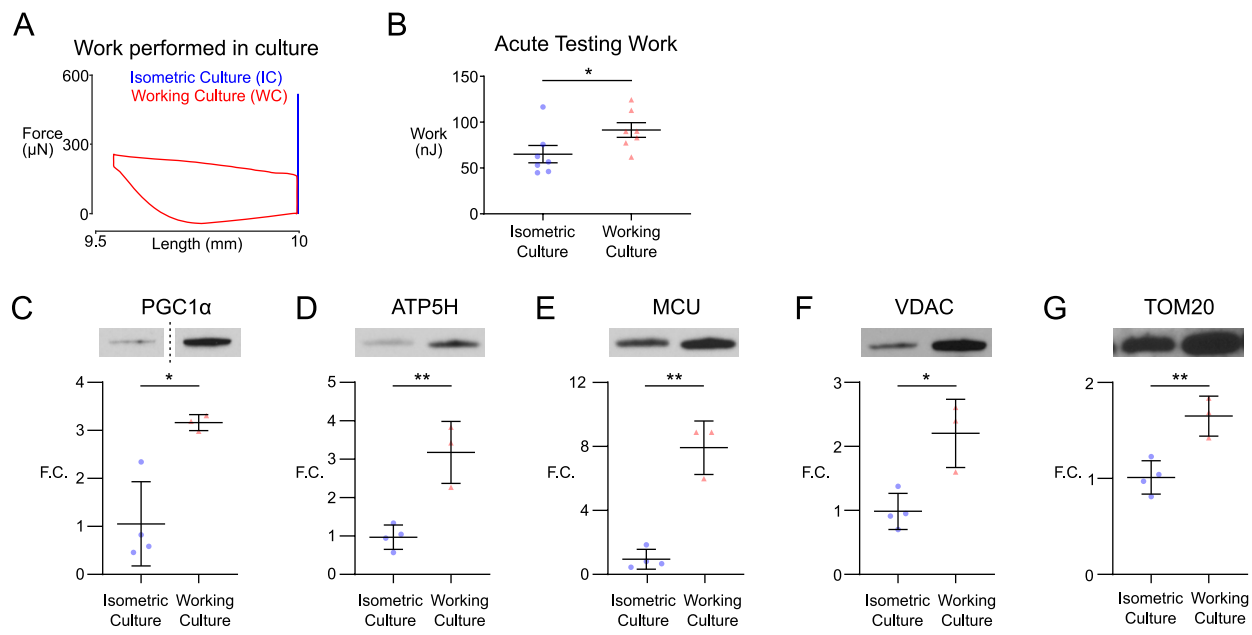


**Figure 3) Working culture conditioned EHTs are more effective at generating contractile work and have higher levels of mitochondrial proteins** (A) Representative force twitches plotted against tissue length. Twitches were collected during acute testing and represent the shortening protocol that each tissue was cultured under. (B) Contractile work generated when EHTs from either group were acutely tested under working culture shortening transients. EHTs cultured under working culture conditions produced significantly higher contractile work compared to EHTs cultured under isometric conditions. (\* $P < 0.05$  for 2-tailed unpaired t-test,  $n = 7$  in each condition) (C-G) Immunoblots probed for levels of PPARγ coactivator 1 α (PGC1α), ATP synthase (ATP5H), mitochondrial calcium uniporter (MCU), voltage-dependent anion channel (VDAC), mitochondrial import receptor subunit20 (TOM20) reveal significantly higher levels in EHTs cultured under working culture. (fold change normalized to isometric; \* $p < 0.05$ , \*\* $p < 0.01$  for 2-tailed unpaired t-test,  $n = 4$  isometric culture;  $n = 3$  working culture)

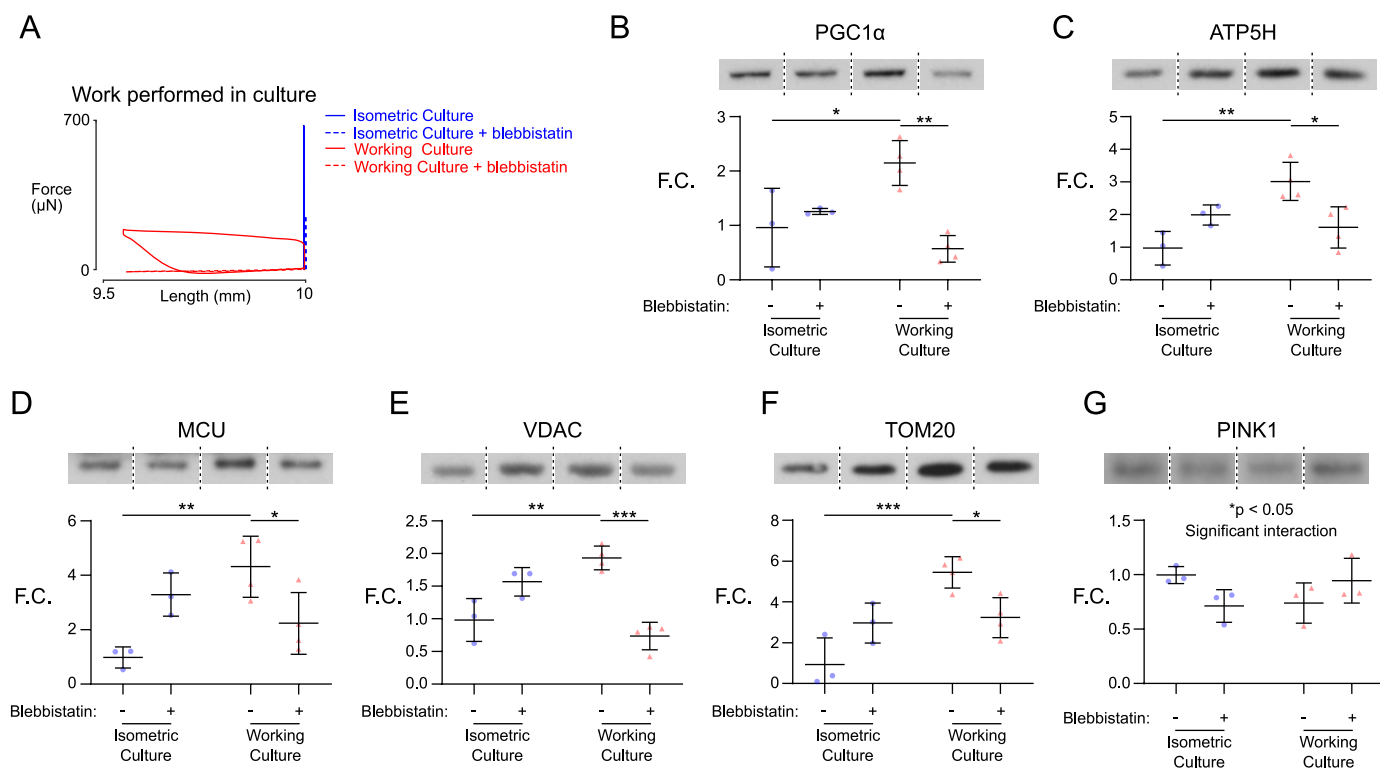


**Figure 4) Increased levels of mitochondrial proteins in working culture EHTs are attenuated by a myosin ATPase inhibitor. (A)** Representative force twitches plotted against tissue length. Twitches were collected during acute testing and represent the shortening protocol that each tissue was cultured under. **(B-F)** PGC1 $\alpha$ , ATP5H, MCU, VDAC, TOM20 protein levels were significantly increased in EHTs cultured under working conditions compared to EHTs cultured isometrically. Blebbistatin treatment significantly reduced protein levels in working culture EHTs. **(G)** PINK1 protein levels showed significant interaction between blebbistatin treatment and culture conditions. (fold change normalized to untreated isometric; n = 3, 3, 4, 4 for IC, IC+blebbistatin, WC, WC+blebbistatin respectively, 2 way ANOVA with Tukey multiple comparisons test \*p < 0.05, \*\*p < 0.01, \*\*\*p < 0.001).



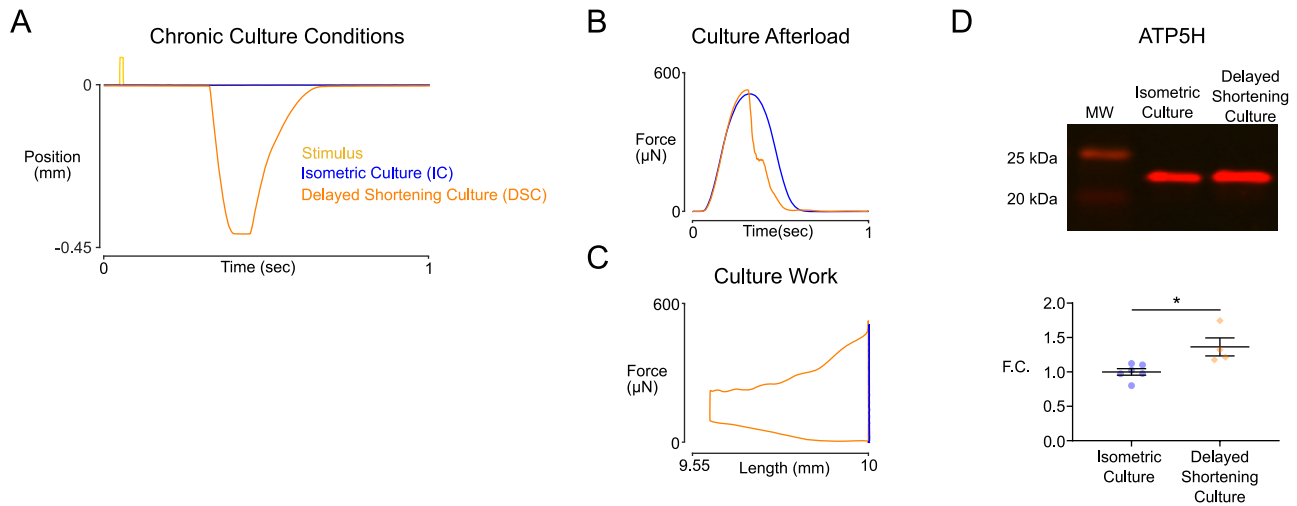


**Figure 5) Training regimes with similar peak afterloads but different work outputs, result in different levels of mitochondrial mass (A)** Position of the spring arm through a single culture cycle. Delayed shortening culture (DSC) initiates shortening concurrent with peak tension, resulting in similar maximal afterload compared to isometric culture, but with increased contractile work. **(B)** Force twitches collected during acute testing demonstrate EHTs from either group experience similar maximal afterload. **(C)** Representative force twitches plotted against tissue length. Twitches were collected during acute testing and represent the increased contractile work EHTs generated in DSC compared to IC. **(D)** EHTs cultured under DSC have increased immunoblot levels of ATP5H (fold change normalized to isometric; \*p < 0.05 for 2-tailed unpaired t-test, IC [n = 6], DSC [n = 4]).

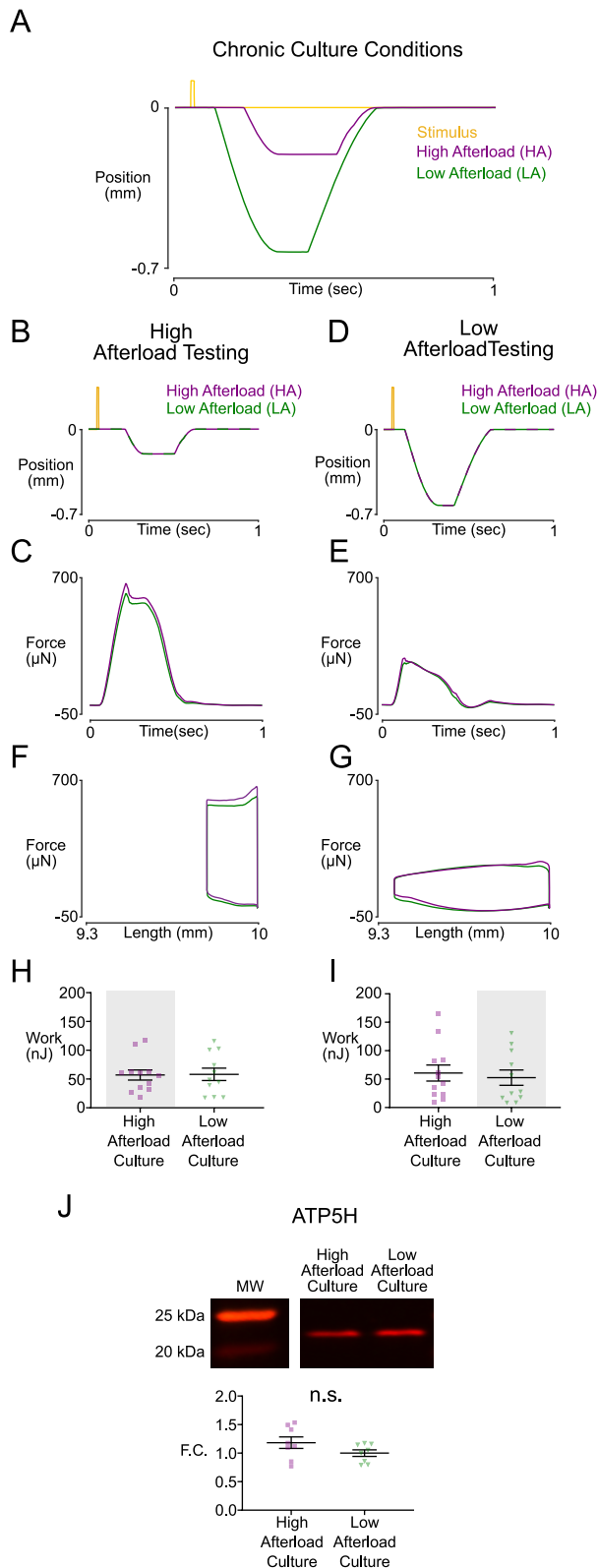
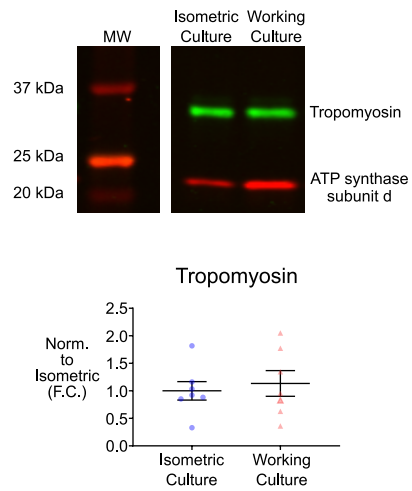
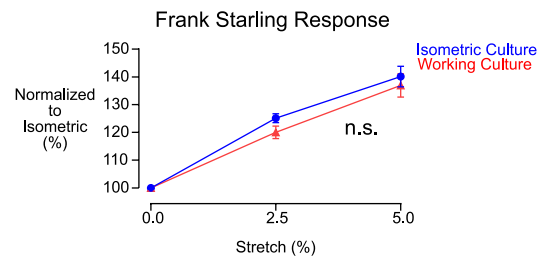


**Figure 6** EHTs subjected to different training regimes with similar work outputs, maintain similar levels of mitochondrial mass **(A)** Position of the spring arm throughout a single culture cycle. High afterload culture (HA) transient is delayed in time and of smaller magnitude compared to Low afterload culture (LA) which results in EHTs contracting against higher load. **(B)** Representative transients of tissue length during acute HA testing after seven days of culture under chronic conditions. **(C)** Representative force twitches collected during acute testing while EHTs underwent the HA shortening protocol represented in Fig 2B. **(D)** Representative transients of tissue length during acute LA testing after seven days of culture under chronic conditions. **(E)** Representative force twitches collected during acute testing while EHTs underwent the LA shortening protocol represented in Fig 2D. **(F)** Representative work loops collected during acute HA testing. **(G)** Representative work loops collected during acute LA testing. **(H)** EHTs generated similar levels of contractile work irrespective of chronic culture conditions during acute HA testing. (HA culture  $n = 12$ , LA culture  $n = 11$ ) **(I)** EHTs generated similar levels of contractile work irrespective of chronic culture conditions during acute LA testing. (HA culture  $n = 12$ , LA culture  $n = 11$ ) **(J)** EHTs from either culture condition had similar immunoblot levels of ATP5H ( $n = 8$  in each condition).

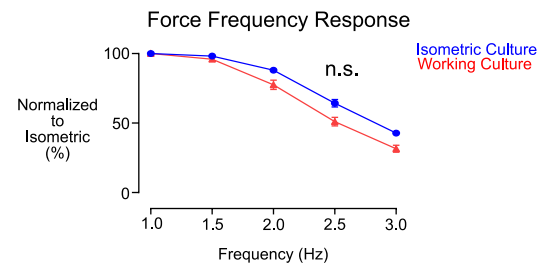
**A**



**B**

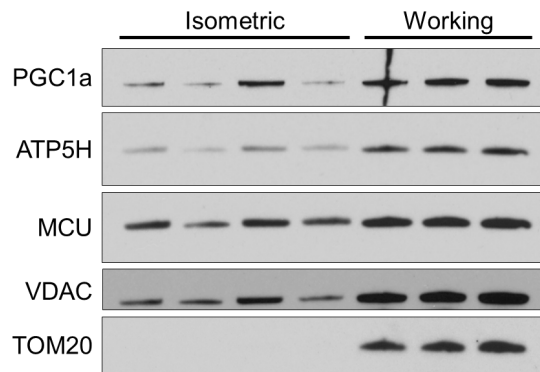


**C**

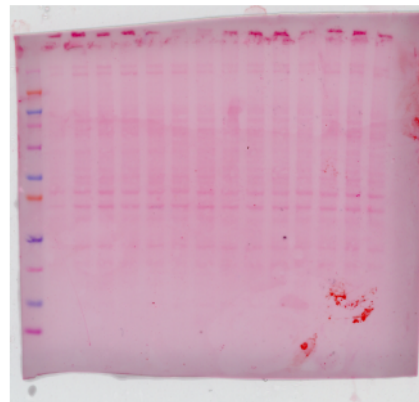
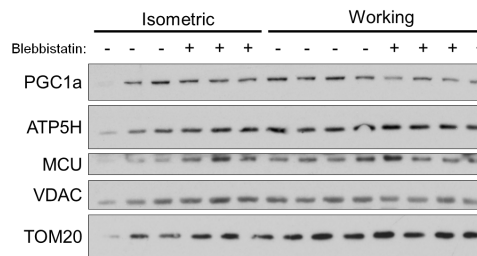


**Supplemental Figure 1** (A) Working culture did not significantly increase levels of tropomyosin. (B) Working culture did not significantly alter Frank-Starling response. (C) Working culture did not significantly alter force - frequency response.

A

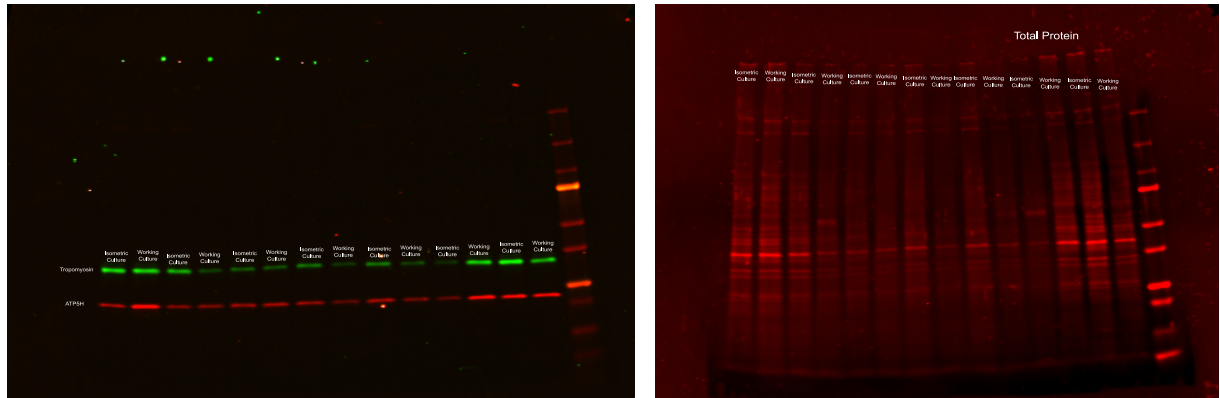


B

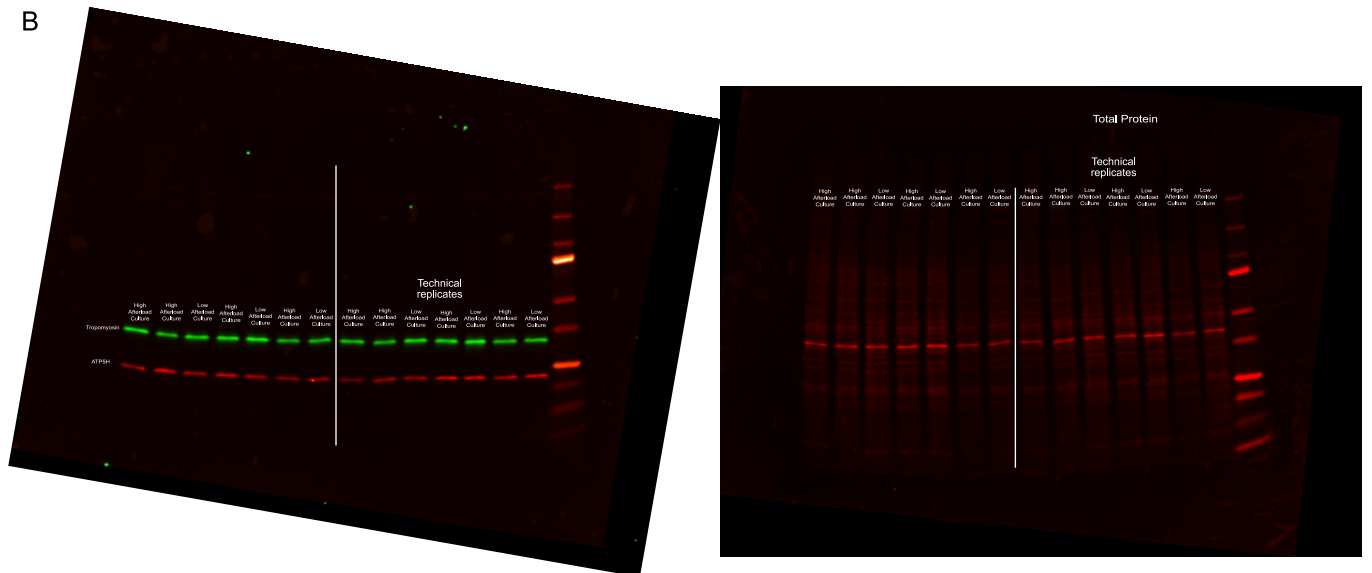


**Supplemental Figure 3) (A-C)** Representative immunoblots for PGC1- $\alpha$ , ATP5H, MCU, VDAC, and TOM20, with associated Ponceau Red Total Protein Stain

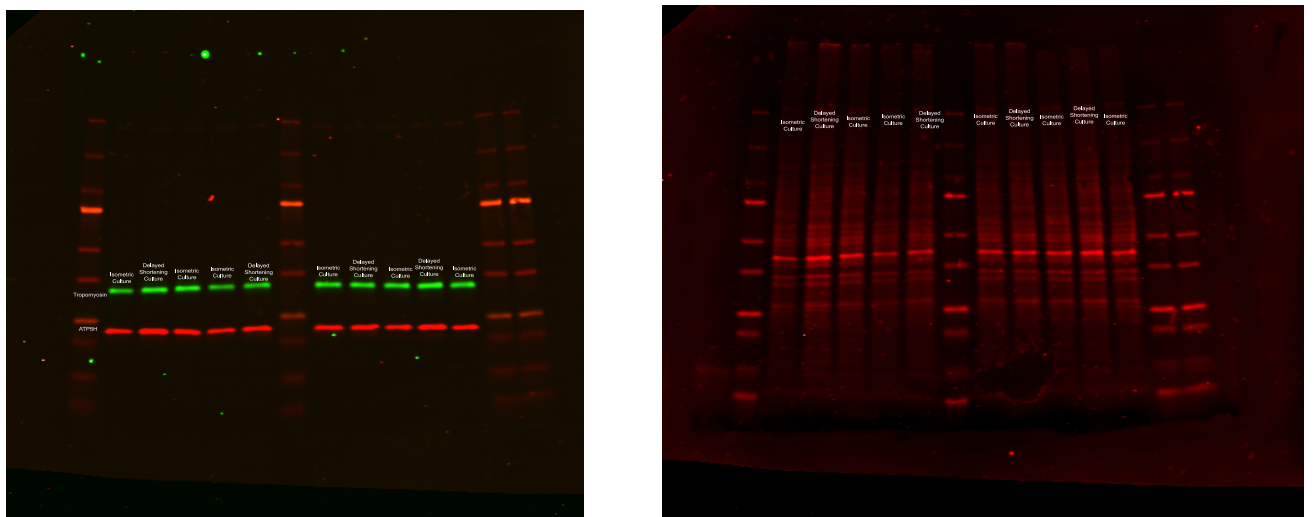
A



B



C



**Supplemental Figure 2) (A-C)** Representative immunoblots for tropomyosin and ATP synthase (ATP5H) with associated Licor Revert Total Protein stains